Hybrid Silicon Photonics Using Oxide-Free Bonding and Nanostructured Effective Materials

H. Benisty, Kristelle Bougot-Robin, Jean-Paul Hugonin, Mondher Besbes, C. Pang, Anne Talneau

Hybrid Silicon Photonics Using Oxide-Free Bonding and Nanostructured Effective Materials

Henri Benisty[1], K. Bougot-Robin[1], J.-P Hugonin[1], M. Besbes[1], C. Pang[1], and A. Talneau[2]
[1]Institut d'Optique Graduate School, Laboratoire Charles Fabry, F-91127 Palaiseau, France
[2]Laboratoire de Photonique et de Nanostructures, CNRS, F-91460 Marcoussis, France
Tel: (0033) 164533286, Fax: (0033) 164533318, e-mail: henri.benisty@institutoptique.fr

ABSTRACT
Oxide-free bonding of indium phosphide epitaxial layers onto silicon-on-insulator (SOI) offers good thermal and electrical contact. These properties are retained if guidance engineering of the resulting stack is performed by nanostructuring the silicon layer to produce a lower effective index layer. We discuss the optical characterization of such a system by a simple prism deviation method for a thin stack, or diffraction to the air for a more multimode stack, adding a superperiod to the nanostructure.
Keywords: hybrid silicon photonics, effective index material, internal light source, guidance.

1. HYBRID SILICON PHOTONICS AND NANOSTRUCTURED EFFECTIVE MATERIAL

Photonic integrated circuits (PIC) on silicon-on-insulator (SOI) can be increasingly functional if laser sources on III-V's, *e.g.*, InP-based, are incorporated in them as proposed in the "hybrid evanescent silicon lasers" in 2006 [1]–[5]. In essentially all the published processes, InP is not directly in atomic contact with Si, being separated either by polymer-based bonding (the common process uses "DVSBCB", see [2]) or by more or less thick SiO_2 layers [5,6] that shall prevent electrical conduction, and to a variable degree, thermal conduction.

Recent contributions on heteroepitaxial bonding have demonstrated oxide-free InP/Si interfaces with an atomic scale reconstructed interface thanks to oxide-free surface preparation and oxide-free annealing conditions [7]. Still, the presence of the silicon as the bottom layer, with its high index, has to be managed optically.

For thick low-index spacers between silicon and InP, the system is rather a set of coupled waveguides. The width of guiding structures can then be used to control the fundamental mode position and its shares between the coupled waveguides.

For our case, it is equally interesting to master the mode profiles. This is feasible by effective materials, *e.g.* sub-wavelength periodic hole arrays in silicon, that can lower the effective index. Such holes, forming an anisotropic nanostructured silicon effective index material (NSEIM), are embedded at the end of the bonding process (Fig. 1a). Hence, even though a micrograph assesses their structural integrity (Fig. 1b), an optical characterization of their role as a low index material is welcome. We assess here their guiding properties through effective index determination. In a general case, a channel waveguide can be defined between two stripes of NSEIM making an apparent InP-covered silicon rib waveguide, with more or less shallow holes [8,9]. We study here an even simpler step, the case of a slab geometry without lateral guidance (structure of Fig. 1a, without ridge).

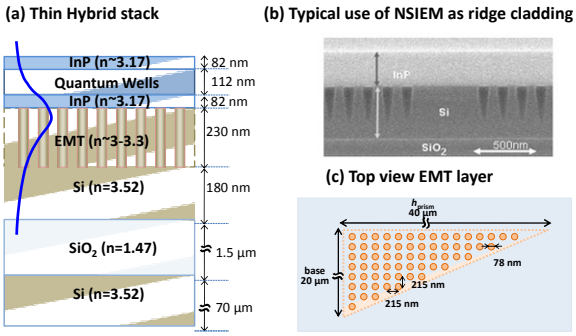

Figure 1: (a) Oxide-free hybrid structure with a nanostructured silicon effective index material (NSEIM: air holes in silicon matrix) and a schematic guided mode profile (b) micrograph of NSEIM used as cladding of Si ridge; (c) top view and details of prism made from NSEIM with air holes of ~80 nm diameter and ~200 nm center to center distance.

As shown in Fig.1c, we use small prisms (20×40 µm typically) of NSEIM illuminated by an internal light source in the III-V and measure the shift of their image caused by prism deviation. We find the indices of NSEIM with typical hole diameters of ~80 nm and period of ~200 nm to be around 3.1 – 3.2, ideally suited to tune the mode profile. We shall discuss later how the homogenization procedure that one is tempted to use to give a physical

account of these indices at modest computational cost has to be adapted to the guiding situation to get a proper result, checked by exact Bloch mode calculations.

We also present preliminary data on another kind of characterisation on a thicker III-V stack, where guidance is multimoded and where the role and position of the fundamental mode is shown to be mastered in a convenient range thanks to the same kind of NSEIM. In that case, the NSEIM has a superperiodic modulation in order to provide reciprocal lattice diffraction carrying the modal information (mode indices and mode-NSEIM interaction) in quite some detail.

2. PRISM CHARACTERIZATION OF NANOSTRUCTURED SILICON IN THIN BONDED STACK

The layer stack discussed here is presented in Fig. 1a. It has a fundamental mode that spans both media, depending on the NSEIM index. We studied the deviation by collecting light at a cleaved edge. As is known from early work on GaAs photonic crystal probe by the ILS (Internal Light Source) method, guided light radiating from a point source and collected at a cleaved edge forms an astigmatic beam, with a focal line at the cleaved edge, and a perpendicular focal line at the geometric image of the source, at a distance d/n_{eff} of the cleaved edge inside the guide (Fig. 2). This is the image that we focus on in our setup. We take as a reference the situation without any specific structure inserted. We then look at the deviation of this vertical line by a series of NSEIM prisms designed with a subwavelength square lattice, and positioned to have their axis along the cleaved edge. Also, they are designed to have as little superperiodic features as possible on their hypotenuses, having directions that correspond to "crystallographic" directions of the square NSEIM. Specifically, hypotenuses directions given as x:y ratio are 1:1, 1:2, 1:3 or 1:4.

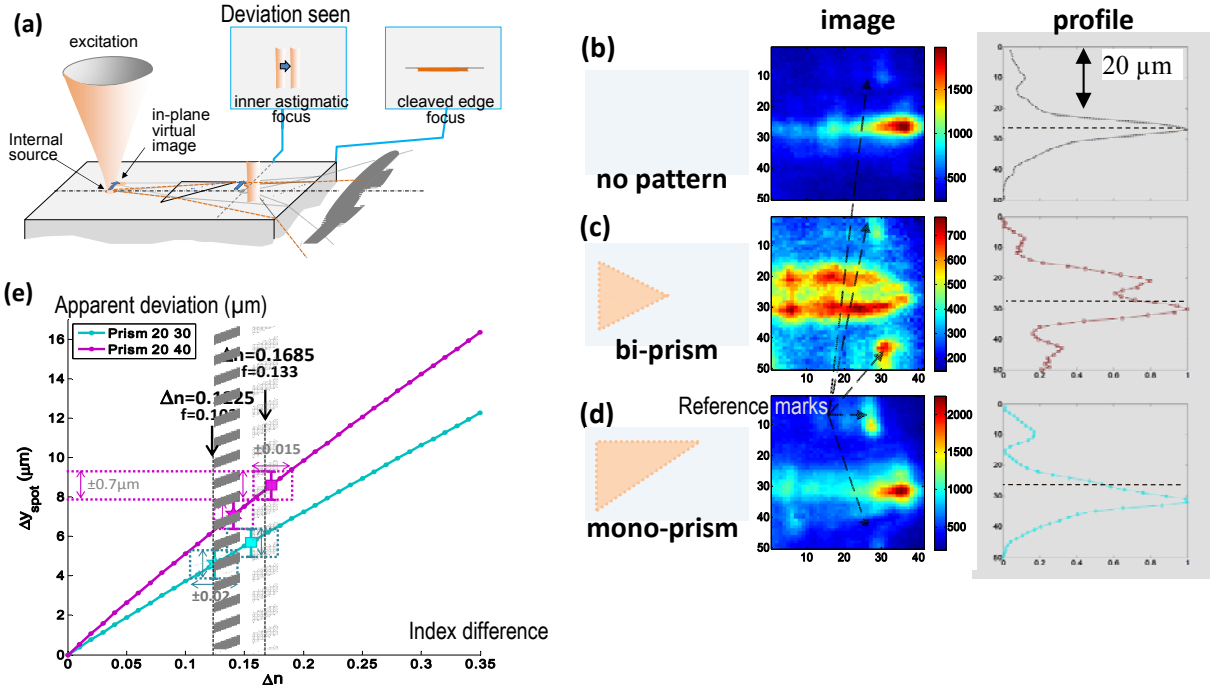

Figure 2: (a) Astigmatism in the beam seen on cleaved edge side; (b) images and averaged profile of virtual source seen without pattern, scale is in µm; (c) same with a biprism 2x (10×20) µm; (d) same with a mono-prism 20×30 µm; (e) spot deviation vs. index difference of prism for two mono-prisms (20×30 µm) and (20×40 µm) and two hole sizes. Grey bands are the aggregate interval from both prism angles, for each hole size.

Typical intensity patterns observed with a camera from single sided "mono-prisms" and double-sided "bi-prisms" are presented in Fig. 2b, 2c, 2d (right panels, scale in µm). For the analysis, we do not need to know very accurately the effective index. The deviation is essentially related to the index difference, and is thus nearly proportional to the air-filling fraction with a factor that grows as the prism acute angle decreases.

Here, the data analysis (Fig. 2e) is done for two hole diameters associated to air filling factors 0.103 and 0.133. They correspond to (diameter, period) pairs of ($d = 74$ nm, $a = 180$ nm) and ($d = 86$ nm, $a = 215$ nm) respectively, this latter close to the subwavelength regime limit. The analysis gives index shifts (associated to TE polarization) of $\Delta n = 0.13$ and 0.16 respectively. It is an interesting value as it makes for NSEIM indices around $n_{\text{NSEIM}} = 3.30$ that then fall between InP and Si indices (resp. $3.17 < n_{\text{NSEIM}} < 3.48$). But this is a simplified view,

as it is actually the mode effective index, about 3.31 without NSEIM, that is shifted by this amount, falling to 3.18 or 3.1. Still; the idea holds that we have synthesized an effective material able to finely tune the coupling.

We will also present a modelling of these values based on the comparison between a 3D Bloch mode calculation and an improved homogenization procedure. Standard homogenization procedures proceed from vertical (v) and horizontal (h) homogenizations in either the h→v or v→h order: either replace NSEIM by a single medium and calculate guidance, or calculate guidance in holes and no holes and average in-plane. For Bloch modes close to the limit of the subwavelength regime, none applies well, and we will show that an averaging based on guided mode profiles suits better. This may provide a simple guide for future users of NSEIM.

3. DISPERSION STUDY FOR NANOSTRUCTURED SILICON IN THICK BONDED STACK

We also wanted to see on a thicker stack whether this NSEIM could be used in a case where the III-V stack is thick enough to accommodate most of the fundamental mode by itself. The idea is that the NSEIM would limit the optical effect of modal attraction by the silicon index, while retaining the good electrical and thermal properties of silicon.

The typical stack we are concerned with, now, has a 500 nm silicon (SOI) basis, on which an oxide-free bonding is made to a stack comprising, from the silicon upward, 100 nm-InP, 400 nm-InGaAsP-SCH-layer with quaternaries and quantum wells, and 820 nm InP buffer (Fig. 3a).

To check the mode dispersion, we prepared an NSEIM of short period (typically a = 150 to 200 nm), with every m-th row (m = 2, 3, 4) having slightly larger holes than the other, typically 86 nm and 66 nm, with a depth of 270 nm. This causes a sizable Fourier component at a relatively small wavevector $G = 2\pi/ma$, able to diffract guided light in the normal direction, as done for photonic crystal extraction studies targeting LEDs [10,11].

We use patterns of typical size 25×70 µm, and we shine the red laser for ILS on the small side of these rectangles, so as to induce guided light propagating mostly along a single given guided direction within the pattern.

We move a thin slit at the back of the collecting lens (NA = 0.42) to sample the various directions of diffracted photoluminescence scattered in the air by the lattice at wavevector G. We are then able to track the dispersion of guided modes, on one side at least since for a given guided wavevector $k_{||}$, this diffraction is detected when $k_{||} - G$ falls in the collection cone. A typical result is presented in Fig. 3b, 3c.

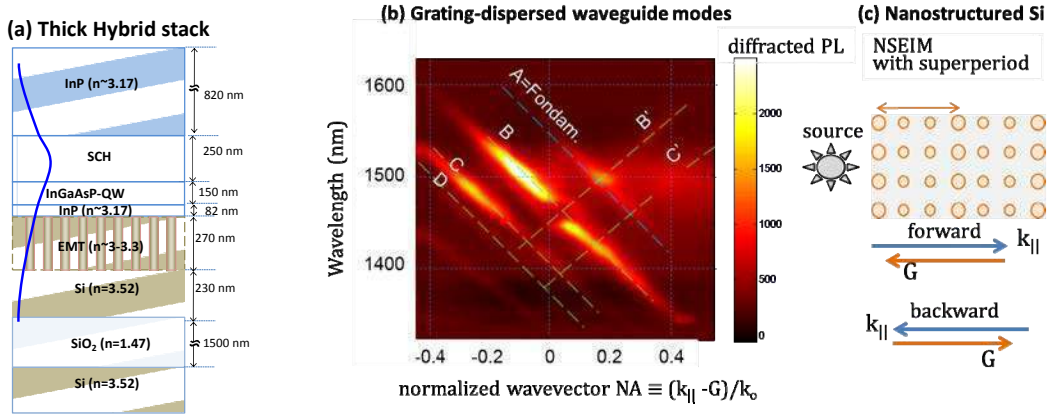

Figure 3: (a) Structure stack with sketch of fundamental mode; (b)Dispersion of guided modes in a thick slab from the diffraction of NSEIM of 160 nm period and actual 480 nm (triple) superperiod, as shown on the right. The fundamental mode is weakly seen. Most modes are diffracted forward waves, but a small amount of backward waves B' and C' are also seen; (c) effective index structure (NSEIM) with superperiodic grating, and detail of involved wavevectors, G is associated with the superperiodicity.

There is no polarization analysis, so we see both TE and TM guided mode diffraction. The exact sequence in terms of intensity depends on the NEIMS characteristic, since it is the product of the quantity of photoluminescence excited by the quantum wells with the overlap with the NSEIM that determines this intensity. Here, the degree of overlap with the NSEIM depends rather strongly here on the NSEIM index in the range 3.1 – 3.4. Modes obtained with a simple fitting are indicated by dashed lines superimposed onto the (wavevector, λ) intensity map.

The most striking feature is that the main mode seen in this way is the second mode with a perfect clear gap, the fundamental mode leading to a very weak signal in comparison, and no detectable gap with our modest 5 nm resolution (related to the slit technique). This is an interesting indication that the fundamental mode is indeed repelled from the silicon to a substantial degree. It thus becomes likely that a laser structure can be fabricated

with a modal structure very close to that of usual proven III-V recipes, while being contacted by silicon having > 80% integrity (thus good thermal and electrical conductivity) on the bottom.

4. CONCLUSION AND PERSPECTIVES

We have shown that nanostructured silicon substrate for oxide-free hybrid silicon photonics could indeed yield the expected modes from such structures, able to finely tune the fundamental mode profile in the presence of the useful silicon bottom, electrically and thermally conductive. Typical nanostructure parameters involve air-filling factors of $f \sim 0.1 - 0.15$ and periods in the range 150 – 220 nm.

We have shown *(i)* characterization by prism deviation in a simple thin slab and *(ii)* extraction of guided light in an angle-selective setup retrieving multiple mode dispersion in a thick slab. The fact that the subwavelength limit is closely tackled in the prism case suggested a simple way to homogenise the system, useful for practitioners. The dispersion study showed that the fundamental mode can be kept mostly in the InP-based part of the system. It thus seems possible to maintain guidance of a form very similar to the classical InP/GaInAsP-based one in spite of the optical presence of the silicon bottom with a high index. Further use of these studies in channel waveguide systems is the next step to get optoelectronic structures of clear interest for applied hybrid silicon photonics.

REFERENCES

[1] A.W. Fang, H. Park, Y.H. Kuo, R. Jones, O. Cohen, D. Liang, O. Raday, M.N. Sysak, M.J. Paniccia, and J.E. Bowers, “Hybrid silicon evanescent devices,” *Mater. Today*, vol. 10, pp. 28-35, 2007.

[2] G. Roelkens, L. Liu, D. Liang, R. Jones, A. Fang, B. Koch, and J. Bowers, “III–V/silicon photonics for on-chip and intra-chip optical interconnects,” vol. 4, p. 779, 2010.

[3] S. Srinivasan, A. W. Fang, D. Liang, J. Peters, K. Bryan, and J. E. Bowers, “Design of phase-shifted hybrid silicon distributed feedback lasers,” *Opt. Exp.*, vol. 19, pp. 9255–9261, 2011.

[4] K. Tanabe, K. Watanabe, and Y. Arakawa, “III–V/Si hybrid photonic devices by direct fusion bonding,” *Sci. Rep.*, vol. 2, 2012.

[5] G. Roelkens, J. Van Campenhout, J. Brouckaert, D. Van Thourhout, R. Baets, P. Rojo-Romeo, P. Regreny, A. Kazmierczak, C. Seassal, X. Letartre, G. Hollinger, J.M. Fedeli, L. Di Cioccio, and C. Lagahe-Blanchardd, “III-V/Si photonics by die-to-wafer bonding,” *Mater. Today*, vol. 10, pp. 36-43, 2007.

[6] J. Van Campenhout, P. Rojo Romeo, P. Regreny, C. Seassal, D. Van Thourhout, S. Verstuyft, L. Di Cioccio, J.M. Fedeli, C. Lagahe, and R. Baets, “Electrically pumped InP-based microdisk lasers integrated with a nanophotonic silicon-on-insulatorwaveguide circuit,” *Opt. Exp.*, vol. 15, pp. 6744-6749, 2007.

[7] A. Talneau, C. Roblin, A. Itawi, O. Mauguin, L. Largeau, G. Beaudoin, I. Sagnes, G. Patriarche, C. Pang, and H. Benisty, “Atomic-plane-thick reconstruction across the interface during heteroepitaxial bonding of InPclad quantum wells on Silicon,” *Appl. Phys. Lett.*, vol. 102, pp. 212101-212103, 2013.

[8] C. Pang and H. Benisty, “Nanostructured silicon geometries for directly bonded hybrid III–V-silicon active devices,” *Photon. Nanostruct.-Fundamentals Appl.*, vol. 11, pp. 145-156, 2013.

[9] C. Pang, H. Benisty, B. Mondher, A. Talneau, and X. Pommarede, "Oxide-free InP-on-Silicon-on-Insulator nanopatterned waveguides: Propagation losses assessment through end-fire and internal probe measurements," *IEEE J. Lightwave Technol.* 32, 1048-1053 (2014).

[10] H. Benisty, J. Danglot, A. Talneau, S. Enoch, J.M. Pottage, and A. David, "Investigation of extracting photonic crystal lattices for guided modes of GaAs-Based heterostructures," *IEEE J. Quantum Electron*. 44, 777-789 (2008).

[11] A. David, H. Benisty, and C. Weisbuch, "Photonic crystal light-emitting sources," *Rep. Prog. Phys*. 75, 12651-12638 (2012).